

EFFECT OF DIFFERENT PLURONIC P123 TRIBLOCK COPOLYMER SURFACTANT CONCENTRATIONS ON SBA-15 PORE FORMATION

Donanta Dhaneswara¹, Nofrijon Sofyan^{1,2*}

¹*Department of Metallurgical and Materials Engineering, Faculty of Engineering, Universitas Indonesia, Kampus UI Depok, Depok 16424, Indonesia*

²*Tropical Renewable Energy Center (TREC), Faculty of Engineering, Universitas Indonesia, Kampus UI Depok, Depok 16424, Indonesia*

(Received: March 2016 / Revised: October 2016 / Accepted: October 2016)

ABSTRACT

Santa Barbara Amorphous-15 (SBA-15) is an interesting mesoporous silica material with highly ordered nanopores and a large surface area. Due to its unique properties, this material has been widely employed in many areas. This study aimed to predict the number of nanopores per gram of SBA-15 material based on an optimum value of surfactant addition at the desired number of nanopores. For this purpose, SBA-15 was synthesized via a sol-gel process using tetraethyl orthosilicate (TEOS, $\text{Si}(\text{OC}_2\text{H}_5)_4$) as a precursor and pluronic P123 triblock copolymer surfactant ($\text{EO}_{20}\text{PO}_{70}\text{EO}_{20}$, EO = ethylene oxide, PO = propylene oxide) as a template. There were five different surfactant concentrations, namely 0.35, 2.50, 2.70, 3.00, and 3.30 millimoles, used with a fixed concentration of TEOS. The characterization was performed using small-angle x-ray scattering (SAXS), adsorption-desorption (BET), and transmission electron microscopy (TEM). The results showed that the surfactant concentration did not affect the crystal structure, although an increase in the surfactant concentration linearly correlated with an increase in the surface area. The shape and size of the pore diameter tends to be approximately 3 nm, as characterized using BET adsorption-desorption. The optimum concentration of surfactant for the formation of mesoporous SBA-15 material was 2.70 millimoles. The value obtained in this study was in accordance with the calculated value, indicating that the theoretical calculations can be used to experimentally predict the number of pores.

Keywords: Mesopores; Pluronic P123; SBA-15; Surfactant; Template

1. INTRODUCTION

Porous materials can be classified as either microporous ($d < 2$ nm), mesoporous (2 nm $< d < 50$ nm), or macroporous ($d > 50$ nm) (Gregg & Sing, 1982). Mesoporous materials have unique characteristics, namely their high surface area and wide range of potential applications (Andriyani et al., 2013). In terms of the application, however, there exists a distinction in the performance criteria required for the use of a particular mesoporous material for a certain application. For example, the performance criteria required for a good absorbent include the absorption capacity, being non-toxic, having a competitive price, and proven effectiveness in absorbing selected materials (Lu & Zhao, 2004; Porter, 1991; Zhao et al., 1998, Göltner et al., 1998).

One type of mesoporous material is Santa Barbara Amorphous-15 (SBA-15), which has a

*Corresponding author's email: nofrijon.sofyan@ui.ac.id, Tel. +62-21-786-3510, Fax. +62-21-787-2350
Permalink/DOI: <https://doi.org/10.14716/ijtech.v7i6.3412>

porous honeycomb structure (Zhao et al., 1998). Pure SBA-15 has a hexagonal structure, with a diameter of 8.9 nm and a wall thickness of 3.1 nm (Zhang et al., 2005). In this material, differences in the composition of the constituent material will cause differences in the pore diameter and wall thickness. The high number of irregular micropores could be responsible for the high surface area of SBA-15 ($650 \text{ m}^2/\text{g}$) (Zhao et al., 1998). Theoretically, the structure has a specific surface area of $204 \text{ m}^2/\text{g}$, assuming that 70% of the area of SBA-15 is due to the microporosity within the inorganic walls (Stevens et al., 2006; Rahmat et al., 2010).

SBA-15 could also have regular cylindrical channels arranged in a hexagonal structure, with a diameter of 5–30 nm, and the solid's volume is only 30% of the total number of pores (Ravikovitch & Neimark, 2001). Further, SBA-15 synthesized from block copolymers will generate 2D tubular channels. In the synthesizing process, SBA-15 can be made or prepared with a pore size of up to 30 nm, which results in a more stable structure because it has thicker pore walls while the pore size decreases to being nano-sized (Zhao et al., 2000).

The synthesis of SBA-15 through triblock copolymer templates has gained significant attention because of the ease of the process and its widespread application. One of the templates used for this purpose is pluronic P123, a triblock copolymer with a chemical formula of EO₂₀PO₇₀EO₂₀, EO = ethylene oxide and PO = propylene oxide (Ruthstein et al., 2003, Ruthstein et al., 2006). This surfactant has been used for templating purposes due to its having similar properties to those of hydrocarbon surfactants. It will form micelles when placed in a selective solvent such as water, in addition to its capability for forming both spherical and cylindrical micelles (Wanka et al., 1994).

In this study, the synthesis of SBA-15 was performed via a sol-gel process using tetraethyl orthosilicate (TEOS) as a precursor and different concentrations of pluronic P123 triblock copolymer surfactant as a template. Further, we developed a formula to calculate the number of pores obtained based on the optimum pluronic P123 surfactant concentration for synthesizing SBA-15 at the desired number of pores. The effect of different pluronic P123 triblock copolymer surfactant concentrations on the pore formation, as well as the prediction of the number of pores obtained in the synthesized material based on the calculation, are reported and discussed in detail.

2. EXPERIMENTAL SETUP

2.1. Material Preparation

The synthesis of SBA-15 involves several steps. First, three different solutions were prepared. For the first solution, 5 ml of ethanol was added to 31.25 grams of TEOS (E-Merck) and then stirred for 30 minutes at room temperature. For the second, 10 ml of HCl (E-Merck) was added to 5 ml of ethanol, while for the third solution, a mixture of 50 ml of distilled water and 10 ml of ethanol was prepared. Secondly, the second and third solutions were mixed and stirred for 30 minutes at room temperature before being added to the first solution and stirred for another 30 minutes. The mixed solution was then refluxed at 50–60°C for 2 hours. Thirdly, in terms of the triblock copolymer surfactant concentration, the addition was made in accordance with the work of others, except for the concentrations of 86.2 μmol (Ruthstein et al., 2006) and 689 μmol (Zhao et al., 1998), which were replaced by different weights of pluronic[®] P123 triblock copolymer surfactant (BASF Corp., USA) to form different concentrations, namely 0.35, 2.50, 2.70, 3.00, and 3.30 millimoles. The surfactant was added to a mixture of 25 ml of ethanol and 10 ml of HCl. The final step was the drop-wise addition of the refluxed TEOS into the pluronic 123 solution, which was then stirred until thickened and the gel was formed. The gel was heated at 100°C for an hour and then calcined at 400°C for 5 hours. The product was then ready for characterization using small-angle x-ray scattering (SAXS, Shimadzu XRD-6000), a

particle size analyzer (Sympatec), adsorption-desorption (Quantachrome), and transmission electron microscopy (TEM, JEOL JEM 2010).

2.2. Pore Calculation

In order to predict the number of pores formed following the synthesis, the density and the average particle size of the material first needed to be measured. In this study, the density (ρ) measurement showed that the product had an average density of 2.2 g/cm^3 , the particle size (S_p) measurement showed an average size of $20 \text{ }\mu\text{m}$, while determining the pore size distribution using adsorption-desorption showed an average pore diameter (D) of 3 nm . Assuming a cubic particle shape, the particle volume (V_p) would be $(20 \text{ }\mu\text{m})^3$ or equal to $8 \times 10^{-9} \text{ cm}^3$. To calculate the mass of a particle (M_p), the formula $M_p = \rho \times V_p$ will result in $1.76 \times 10^{-8} \text{ gr}$. Based on this value, the number of particles (n_p) in one gram of SBA-15 would be one gram/ 1.76×10^{-8} or 5.68×10^7 particles. Furthermore, the pore volume (V_{pr}) can be calculated using the simple formula presented in Equation 1:

$$V_{pr} = \pi \left(\frac{D}{2} \right)^2 S_p \quad (1)$$

where V_{pr} is the pore volume, D is the pore diameter, and S_p is the particle size. The number of pores in one gram (n^*) of SBA-15 is then calculated using Equation 2:

$$n^* = n_p \times n' \quad (2)$$

where n' is the number of pores in one particle, which can be calculated using Equation 3:

$$n' = \frac{V_p}{V_{pr}} \quad (3)$$

Assuming that the area of a pore would be the same as that of a cylindrical blanket surface area, the open surface pore area in one gram (S_A) of SBA-15 can be calculated using Equation 4:

$$S_A = n^* \left(2\pi \frac{D}{2} \times S_p \right) \quad (4)$$

3. RESULTS AND DISCUSSION

The small-angle x-ray scattering (SAXS) pattern is presented in Figure 1. Three main peaks can be observed in the figure, namely (100), (110), and (200), for all the surfactant concentrations. In general, the synthesized SBA-15's x-ray scattering patterns show that these three major peaks are in agreement with those obtained in other studies (Su et al., 2005). With these three points corresponding to the main reference peaks, the peaks represent quite convincing evidence that the result of the synthesized material is SBA-15 with a hexagonal structure. No other peaks from other phases are found in the patterns; however, with the increase in surfactant concentration, the peaks display a tendency to shift to a lower angle. As can clearly be seen in the figure, the peak (100) from the surfactant concentrations of 3.00 and 3.30 millimoles shifts toward a lower angle when compared to those of the other three concentrations. The same is true for the peaks (110) and (200) from the surfactant concentrations of 2.50, 2.70, 3.00, and 3.30 millimoles when compared to that of the surfactant concentration of 0.33 millimoles. This shifting is likely due to the change in the lattice parameters whereby the increase in surfactant

concentrations results in the expansion of the lattice parameters and thus shifts the peaks toward lower angles.

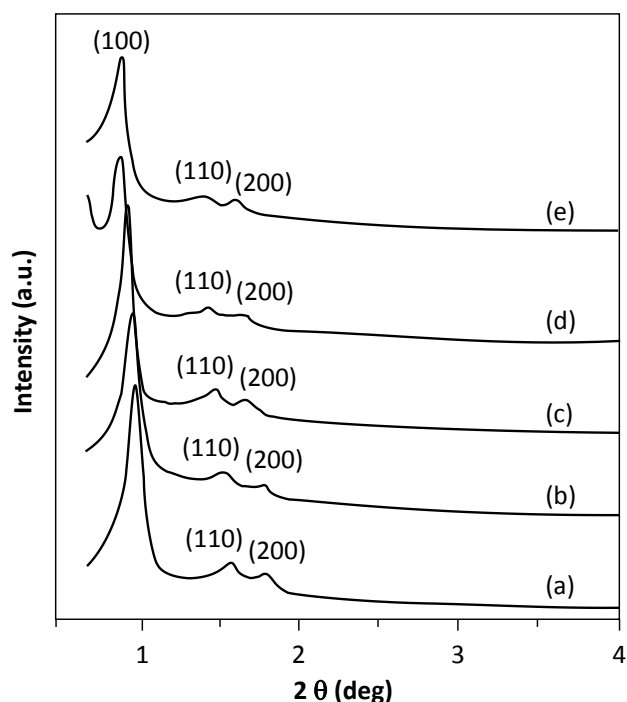


Figure 1 Small-angle x-ray scattering patterns of SBA-15 at various pluronic P123 surfactant concentrations: (a) 0.33; (b) 2.50; (c) 2.70; (d) 3.00; and (e) 3.30 millimoles

The pore properties of the synthesized SBA-15 as characterized using a nitrogen adsorption-desorption isotherm at a temperature of 77°K are given in Figure 2a, while the pore size distribution curves are presented in Figure 2b.

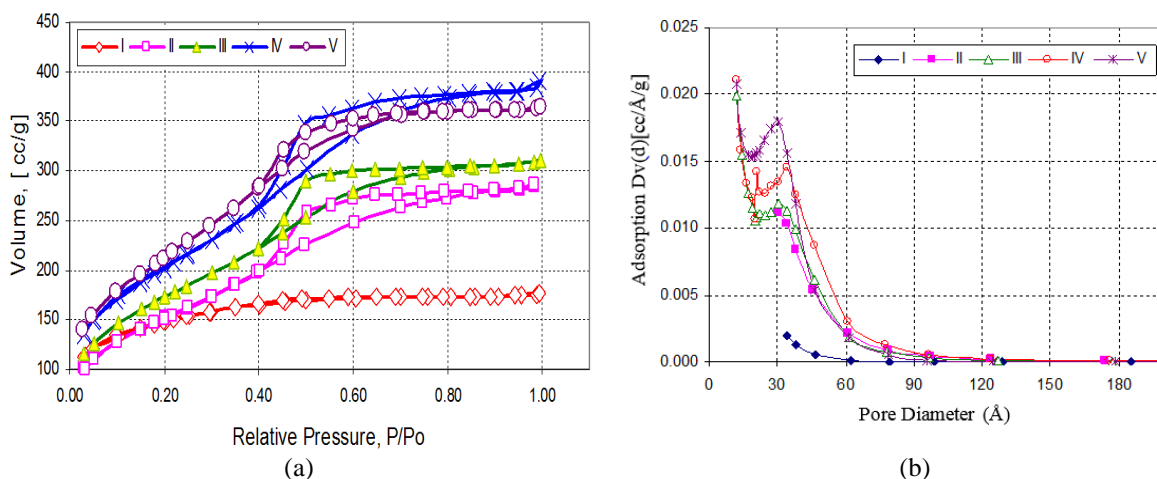


Figure 2 Adsorption-desorption isotherm (a) and pore size distribution curves (b) of the SBA-15 material at different surfactant concentrations, namely: (I) 0.35, (II) 2.50, (III) 2.70, (IV) 3.00, and (V) 3.30 millimoles

As can be seen from the Figure 2a, the sample with a surfactant concentration of 0.35 millimoles has almost no hysteresis loop, or else it is too small to observe, even though the trend still indicates a mesoporous-type material. The other four concentrations show adsorption-

desorption isotherms with a hysteresis loop in the relative pressure of (P/P₀) 0.4 to 0.9. This indicates that the SBA-15 materials obtained from these concentrations are mesoporous materials with a type IV adsorption-desorption isotherm (Gregg & Sing, 1982). These hysteresis loops are primarily caused by cylindrical pore channels, pores formed from inter-particle gaps (slit pores), and/or pores from the gaps along the particle plate (Rouqe-Malherbe, 2007).

In terms of the pore diameter, as can be seen from Figure 2b, save for the surfactant concentration of 0.35 millimoles, all the relative average pore diameters are dominant at a range of 3 to 5 nm. With regard to the surfactant concentration of 0.35 millimoles, it seems that the size distribution does not have a specific peak, meaning that it might not have a pore or else it could be a micropore-type material, which cannot be detected by the current nitrogen adsorption-desorption isotherm. In terms of the effect of the surfactant concentration on pore formation, Figure 2b shows that there is a tendency toward a slight increase in the pore diameter from 3.0 to 3.5 nm with the increase in surfactant concentration from 2.50 to 3.30 millimoles. At 3.30 millimoles, the distribution of the pore diameter decreases back to 3 nm. In this instance, there would be an optimum concentration of the surfactant available to form pores within the material during the synthesis. There would not be sufficient surfactant to create the pores if the concentration was too low, whereas, on the contrary, if the concentration is too high it could destroy the pores.

The theoretical calculation used in the experimental setup results in a number of pores per gram (n^*) of 3.2168×10^{15} , with a surface area per gram (S_A) of $605.8 \text{ m}^2/\text{g}$. The values of n^* and S_A could then be used as reference values (baseline) to determine the optimum surfactant pluronic P123 concentration for synthesizing SBA-15 at the desired number of pores. The details results of this calculation are given in Table 1. The table presents the experimental results as well as the value obtained from the theoretical calculation at various surfactant concentrations.

Table 1 Different surfactant concentrations result in different surface areas and different numbers of pores/gram in SBA-15

Specimen	P123 (millimole)	Particle size (μm)	Surface area (m^2/gr)	Pore/gram
I	0.35	18.80	482.20	2.56×10^{15}
II	2.50	19.38	534.60	2.84×10^{15}
III	2.70	21.93	598.50	3.10×10^{15}
IV	3.00	21.65	702.10	3.73×10^{15}
V	3.30	19.86	746.70	3.97×10^{15}

From the table, it can be seen that a change in the surfactant concentration will lead to an increase in the number of pores and thus in the surface area. By comparing the increase in the surfactant concentration in the third specimen with the increases seen in specimens IV and V, a prediction can be made as to the degree of self-assembly of the surfactants that form secondary pores (intra-wall porosity). Self-assembly is a process by which molecules orientate or prepare to spontaneously become relatively small components (Thielemann et al., 2011). The driving force behind this self-assembly consists of electrostatic force, hydrophilicity, hydrophobicity, capillarity force, and chemical adsorption (Gao et al., 2013).

The topographic observation of the specimen using TEM can be seen in Figure 3. For technical reasons, the observation was only performed on the SBA-15 specimen with a surfactant concentration of 2.70 millimoles. As can be seen in the figure, the indistinct dark spots on the surface as indicated by the arrows are suspected to be open pores in the form of cylindrical

channel structures. These pores have diameters of about 3 to 5 nm, and this finding is consistent with the results obtained from the adsorption-desorption isotherm data. These pores would be the primary pores and they are usually formed in lamellar and/or cylindrical channel structures arranged in a hexagon to form honeycomb structures (Ravikovitch & Neimark, 2001). This TEM observation is also in agreement with the data obtained from the calculation.

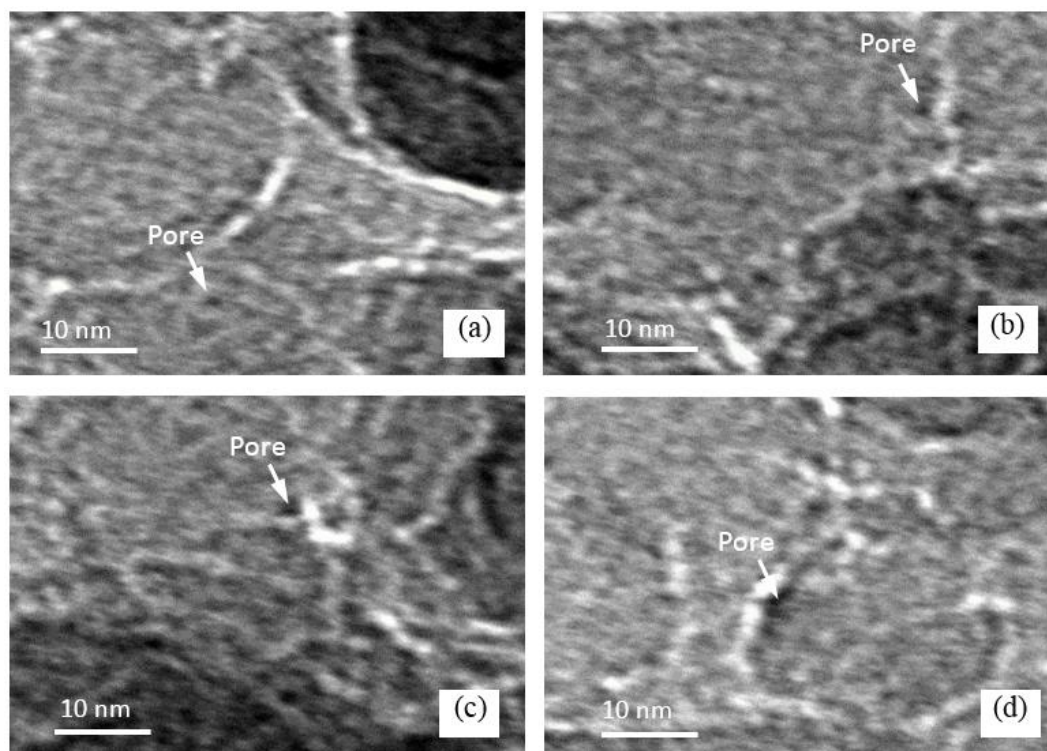


Figure 3 TEM topography of the surface structure of SBA-15 with a surfactant concentration of 2.70 millimoles. With the bar scale of 10 nm shown, the pore diameters are around 3 nm

4. CONCLUSION

By evaluating the crystal structure, surface area, pore diameter, and pore microstructure, it can be concluded that the addition of surfactant variables affects the pore characteristics of SBA-15. Specifically, in this study, an increase in the surfactant concentration increases the surface area of SBA-15. For the surfactant concentration variations ranging from 0.35 to 3.30 millimoles, there is an increase in the surface area ranging from 482.20 m²/g to 746.70 m²/g, with the number of pores per gram ranging from 2.56×10¹⁵ to 3.97×10¹⁵ pores. Further, the formula developed in this research works well and the results are quite convincing. Thus, it could be used to predict the number of pores based on the amount of SBA-15 and the surfactant concentration used during synthesis.

5. REFERENCES

- Andriyani, A., Sembiring, S.B., Aksara, N., Sofyan, N., 2013. Synthesis of Mesoporous Silica from Tetraethylorthosilicate by using Sodium Ricinoleic as a Template and 3-Aminopropyltrimethoxysilane as Co-Structure Directing Agent with Volume Variation of Hydrochloric Acid 0.1 M. *Advanced Materials Research*, Volume 789, pp. 124–131
- Anjum, A., Ilyas, M.U., 2013. *Activity Recognition using Smartphone Sensors*. First Workshop on People Centric Sensing and Communications. Las Vegas

- Gao, C., Zhang, T., Gao, P., Zhao, Y., 2013. Bridged-ferrocene Functionalized Mesoporous SBA-15 Material Prepared via Evaporation-Induced Self-Assembly. *Journal of Porous Materials*, Volume 20(1), pp. 47–53
- Göltner, C.G., Henke, S., Weissenberger, M.C., Antonietti, M., 1998. Mesoporous Silica from Lyotropic Liquid Crystal Polymer Template. *Angewandte Chemie International Edition*, Volume 37(5), pp. 613–616
- Gregg, S.J., Sing, K.S.W., 1982. *Adsorption, Surface Area and Porosity*. Second Edition, London, Academic Press
- Lu, G.Q., Zhao, X.S., 2004. Nanoporous Materials – An Overview. In: *Nanoporous Materials- Science and Engineering*, Edited by G.Q. Lu and X.S. Zhao, Imperial College Press, London, pp. 1–13
- Porter, M.R., 1991. *Handbook of Surfactant*. New York, Chapman and Hall
- R.M.A., Rouque-Malherbe, 2007. *Adsorption and Diffusion in Nanoporous Material*. New York, CRC Press, Taylor & Francis Group
- Rahmat, N., Zuhairi, A.A., Mohamed, A.R., 2010. A Review: Mesoporous Santa Barbara Amorphous-15, Types, Synthesis and Its Applications towards Biorefinery Production. *American Journal of Applied Sciences*, Volume 7(12), pp. 1579–1586
- Ravikovitch, P.I., Neimark, A.V., 2001. Characterization of Micro- and Mesoporosity in SBA-15 Materials from Adsorption Data by the NLDFT Method. *Journal of Physical Chemistry B*, Volume 105(29), pp. 6817–6823
- Ruthstein, S., Frydman, V., Kababya, S., Landau, M., Goldfarb, D., 2003. Study of the Formation of the Mesoporous Material SBA-15 by EPR Spectroscopy. *Journal of Physical Chemistry B*, Volume 107(8), pp. 1739–1748
- Ruthstein, S., Schmidt, J., Kesselman, E., Talmon, Y., Goldfarb, D., 2006. Resolving Intermediate Solution Structures during the Formation of Mesoporous SBA-15. *Journal of American Chemical Society*, Volume 128(10), pp. 3366–3374
- Stevens, W.J.J., Lebeau, K., Mertens, M., van Tendeloo, G., Cool, P., Vansant E.F., 2006. Investigation of the Morphology of the Mesoporous SBA-16 and SBA-15 Materials. *Journal of Physical Chemistry B*, Volume 110(18), pp. 9183–9187
- Su, F., Zeng, J., Bao, X., Yu, Y., Lee, J.Y., Zhao, X.S., 2005. Preparation and Characterization of Highly Ordered Graphitic Mesoporous Carbon as a Pt Catalyst Support for Direct Methanol Fuel Cells. *Chemistry of Materials*, Volume 17(15), pp. 3960–3967
- Thielemann, J.P., Girgsdies, F., Schlögl, R., Hess, C., 2011. Pore Structure and Surface Area of Silica SBA-15: Influence of Washing and Scale-Up. *Beilstein Journal of Nanotechnology*, Volume 2, pp. 110–118
- Wanka, G., Hoffmann, H., Ulbricht, W., 1994. Phase-Diagrams and Aggregation Behavior of Poly(Oxyethylene)-Poly(Oxypropylene)-Poly(Oxyethylene) Triblock Copoly-mers in Aqueous-Solutions. *Macromolecules*, Volume 27(15), pp. 4145–4159
- Zhang, F., Yan, Y., Yang, H., Meng, Y., Yu, C., Tu, B., Zhao, D., 2005. Understanding Effect of Wall Structure on the Hydrothermal Stability of Mesostructured Silica SBA-15. *Journal of Physical Chemistry B*, Volume 109(18), pp. 8723–8732
- Zhao, D., Feng, J., Huo, Q., Melosh, N., Glenn, H., Chmelka, B.F., Stucky, G.D., 1998. Triblock Copolymer Syntheses of Mesoporous Silica with Periodic 50 to 300 Angstrom Pores. *Science*, Volume 279(5350), pp. 548–552
- Zhao, D., Huo, Q., Feng, J., Chmelka, B.F., Stucky, G.D., 1998. Nonionic Triblock and Star Diblock Copolymer and Oligomeric Surfactant Syntheses of Highly Ordered, Hydrothermally Stable, Mesoporous Silica Structures. *Journal of American Chemical Society*, Volume 120(39), pp. 6024–6036
- Zhao, D., Sun, J., Li, Q., Stucky, G.D., 2000. Morphological Control of Highly Ordered Mesoporous Silica SBA-15. *Chemistry Materials*, Volume 12(2), pp. 275–279